

On the oxygen p states in superconducting nickelates

Frank Lechermann

Institut für Theoretische Physik III,
Ruhr-Universität Bochum, D-44780 Bochum, Germany

While key attention in transition-metal oxides is usually devoted to the d states of the transition-metal ion, the $O(2p)$ states usually also carry important physics. We here examine these p states in representatives of the novel superconducting nickelates, as described in realistic dynamical mean-field theory. Since the materials are located on the boundary between Mott-Hubbard and charge-transfer systems, the role of oxygen is expectedly subtle. Strong reduction of doped holes on oxygen and first asymmetry effects are featured in infinite-layer nickelates. A pronounced nature of bridging p_z orbitals is identified in the $\text{La}_3\text{Ni}_2\text{O}_7$ system.

1 Introduction

In late summer 2019, the long-sought discovery of superconductivity in nickel oxides finally opened up a new research field in condensed matter physics. Strontium doping of thin films of so-called infinite-layer NdNiO_2 on SrTiO_3 substrates leads to a superconducting phase below $T_c \sim 15 \text{ K}$ ¹. Early follow up works revealed further similar superconducting scenarios in Sr-doped $(\text{La},\text{Pr})\text{NiO}_2$, as well as in the stoichiometric multilayer compound $\text{Nd}_6\text{Ni}_5\text{O}_{10}$ ². All these low-valence nickelate materials with $\text{Ni}(3d^{9-\delta})$ filling share the fact that the apical oxygens of the basic NiO_6 octahedra are missing.

In early spring 2024, a second class of superconducting nickelates emerged. The bilayer $\text{La}_3\text{Ni}_2\text{O}_7$ was reported superconducting under high pressure $p > 14 \text{ GPa}$ with a much higher $T_c \sim 80 \text{ K}$ ³. Soon after, the trilayer compound $\text{La}_4\text{Ni}_3\text{O}_{10}$ was proven to also show superconductivity in a similar pressure regime, but with an again lower $T_c \sim 20 \text{ K}$ ⁴. Those nickelates with $\text{Ni}(3d^{8-\delta})$ filling have intact NiO_6 octahedra.

From the start, the superconducting nickelates were compared to high T_c cuprates, because of their proximity in the periodic table and the akin building block of square-lattice transition-metal (TM) oxide planes. However the degree of similarity in terms of physical properties and superconducting nature is still under heavy debate. For detailed representations of the known and discussed features from experiment and theory, we here refer to available early review articles, e.g. Refs. 5–8. One key issue concerns the number of relevant $\text{Ni}(3d)$ frontier orbitals. While there is strong consensus that only the $d_{x^2-y^2}$ TM orbital is of crucial importance in high- T_c cuprates, in general electronic properties of nickelates the complete e_g subshell $\{d_{z^2}, d_{x^2-y^2}\}$ has to be taken into account. At least for the $d^{8-\delta}$ bilayer and trilayer superconducting compounds, a pure single-orbital cuprate(-like) physics seems very unrealistic both from theory and experiment.

Yet the present work does not focus on the detailed characteristics of the $\text{Ni}(3d)$ degrees of freedom. Instead, it takes a deeper look on the behavior of the $O(2p)$ states in the normal state of superconducting nickelates. While the impact of those p states is more subtle, some interesting aspects may still be revealed and learned from first-principles many body theory. We show that the ligand-hole concept, i.e. deviation from the simplistic purely-ionic O^{2-} picture, is a steady companion in these nickel oxides. It asks to be properly

considered, weighed and addressed, both in the low- and high-energy regime. Noteworthy differences in the energetics and the occupation between p_z and $p_{x,y}$ orbitals are observed.

2 Theoretical Background and Approach

The physics of strong electron correlation in materials such as the superconducting nickelates asks for a proper treatment of both, the realistic band theoretical aspect as provided by the chemical bond in the solid, as well as the explicit many-body aspect of interacting electrons. The state-of-the-art approach to realize such a faithful description is given by the hybrid scheme of combining density functional theory (DFT) with dynamical-mean field theory (DMFT), i.e. the so-called DFT+DMFT method (see e.g. Refs. 9 for the basics). There usually, the transition-metal (TM) sites are the centre of attention, serving as DMFT impurities, while the description of the ligand states remains on the DFT level (albeit surely coupled to the strongly correlated TM sites). However in nickelates, we are most often dealing with possible low-energy states of strongly hybridized TM($3d$)-O($2p$) character. This is different compared to early TM oxides, e.g. titanates or vanadates, where the O($2p$) states only weakly hybridize into the low-energy physics and the systems reside more robustly in the so-called Mott-Hubbard regime of correlated materials¹⁰. There, the effective Hubbard U_{eff} is smaller than the charge-transfer energy $\Delta = \varepsilon_d - \varepsilon_p$, with $\varepsilon_{d,p}$ describing the average onsite energy of the TM($3d$) and O($2p$) states.

From a basic quantum-scattering perspective, TM($3d$) states are difficult to handle by sole band theory. Because the $3d$ orbitals are not orthogonalized on lower lying d orbitals, their electrons approach the ion core region quite easily. This leads to the observed strong competition between the electrons' itinerant vs. localized character in the solid state, giving rise to the plethora of correlation effects emerging from TM($3d$) compounds. Notably, also O($2p$) is not orthogonalized on lower lying p states and therefore the electrons are also more localized than $3p$ or even higher p electrons. While due to the high electronegativity, smaller orbital Hilbert space and strong bonding tendencies, the quantum-fluctuating character of O($2p$) is much less pronounced than TM($3d$), correlation effects beyond DFT can still matter also from that perspective. This may especially be true when O($2p$) plays a more prominent role in the low-energy regime of late TM oxides. Therefore on the methodological level, the differentiation in the correlation treatment of TM($3d$) and O($2p$) states may be too severe in standard DFT+DMFT for certain classes of materials. And understandably, issues such as the pd splitting, p -induced renormalization effects or intriguing ligand-mediated exchange might not be well described. There are several ideas in going beyond this strong-differentiation treatment, for instance by combining DMFT with the GW method¹¹⁻¹³ or with screened-exchange formalisms¹⁴. Our choice builds up on introducing the self-interaction correction (SIC) scheme for oxygen orbitals on the pseudopotential level¹⁵, to be utilized in a complete charge-selfconsistent DFT+DMFT framework¹⁶. This so-called DFT+sicDMFT scheme¹⁷ improves the pd -splitting description and handles p -induced correlation effects (e.g. explicit oxygen-mediated band narrowing). The SIC naturally enables correlation effects free from the need of symmetry breakings, but is numerically much less demanding as e.g. GW+DMFT.

In the present context of superconducting nickelates, the Ni sites act as DMFT quantum impurities and Coulomb interactions on oxygen enter by the SIC-modified pseudopotentials. The DFT part consists of a mixed-basis pseudopotential code¹⁸⁻²⁰ and SIC is applied

to the $O(2s, 2p)$ orbitals via weight factors w_p . While the $2s$ orbital is fully corrected with $w_p = 1.0$, the choice^{15,17,21} $w_p = 0.8$ is used for $2p$ orbitals. Continuous-time quantum Monte Carlo in hybridization-expansion scheme²² as implemented in the TRIQS code^{23,24} solves the DMFT problem. A five-orbital Slater-Hamiltonian, parameterized by Hubbard $U = 10$ eV and Hund exchange $J_H = 1$ eV²¹, governs the correlated subspace defined by $Ni(3d)$ projected-local orbitals²⁵. Crystallographic data are taken from experiment.

3 General remarks on oxygen p states in nickelates

Nickelates are special in their correlation physics. While cuprates are usually located in the strong charge-transfer regime, i.e., the effective Hubbard U_{eff} is way larger than the charge-transfer energy Δ , the nickelates are closer to a competing regime of Mott-Hubbard versus charge-transfer dominance. Note that the calculational $U > U_{\text{eff}}$ in DFT+sicDMFT, since further screening processes occur in the charge-selfconsistent many-body approach. The leveling of U_{eff} and Δ leads to a subtle role of $O(2p)$ regarding the interplay of its low- and high-energy electronic character. In a Mott-Hubbard system, the oxygen p states reside in their localized high-energy being, whereas their itinerant nature is most vital in a charge-transfer system. The subtlety is also reflected in the ligand-hole physics of in fact many nickelates. Figure 1 displays the evolution of the charge-transfer energy Δ and the amount of holes in the oxygen $2p$ shell (per single O ion) h_p from high to low valence of Ni in given Ruddlesden-Popper(-like) nickelates. The data for Δ is computed from DFT+sic, i.e. a conventional Kohn-Sham calculation but using the SIC-modified oxygen pseudopotential. As the result of the fully-interacting problem, the data for h_p is obtained from DFT+sicDMFT.

From formal Ni^{3+} to formal Ni^{2+} , the value of Δ rises more or less monotonically, as expected from the ionic physics of these elements. This means, $O(2p)$ and $Ni(3d)$ split energetically stronger when the Ni valence becomes smaller. The filling of the $O(2p)$ shell

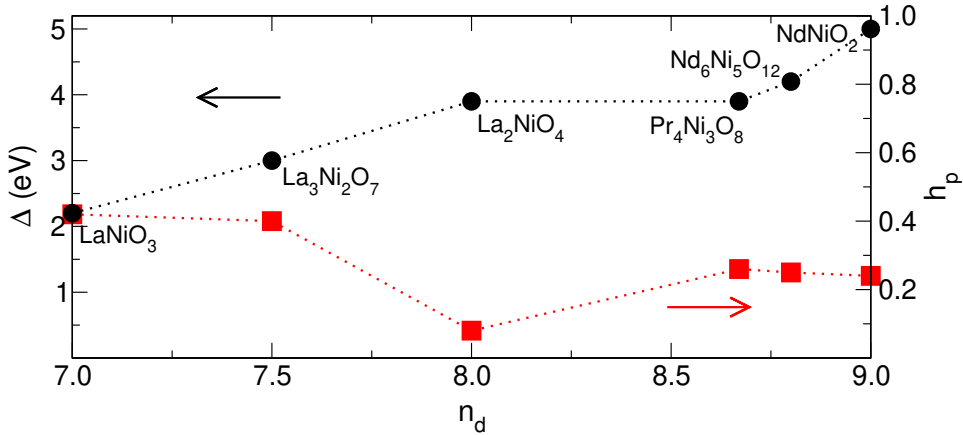


Figure 1. Charge-transfer energy Δ and $O(2p)$ hole content h_p for selected standard ($n_d \leq 8$) and reduced ($n_d > 8$) Ruddlesden-Popper nickelates with formal $Ni(3d)$ count n_d . Note the plateau-like region in Δ for $8 < n_d < 8.67$.

is set by Δ , hoppings as well as by the Coulomb interactions in the system, most notably the on-site Coulomb U_{pp} and the inter-site Coulomb U_{pd} . In other words, the standard identification of O^{2-} in oxides is not necessarily always true. For instance, this ionic configuration amounts to a large Coulomb penalty within $O(2p)$, which should be properly considered within the full group of mechanisms on the given lattice that eventually fix h_p . Intuitively, we expect for small Δ a larger h_p since electrons can more easily be transferred between sites, i.e. the degree of covalency is increased. Indeed, for formal Ni^{3+} the hole content on oxygen is substantial, amounting to roughly one charge unit within the unit cell. This ligand-hole $3d^8L$ state is well-known for nickelates with nominal higher valence than the ideal $2+$ oxidation in the solid²⁶. However, as shown in Fig. 1 this hole content does not fall to zero for less than nominal Ni^{2+} . The situation is more intriguing due to the various electronic mechanisms at play, leading to quite some finite covalency also for the lower-valence nickelate. Again, the O^{2-} fully-ionic picture is usually fine as a first guess, but by no means always the full truth in a complex realistic many-body compound. This limit is here only reasonably-well reached for the Mott-charge-transfer insulator La_2NiO_4 . While the existing basic Mott vs. charge-transfer schemes provide good principle guidance, the actual charge distribution in a concrete material is quite sophisticated, building up on the interplay of a multitude of physical process (in a Hilbert space enclosing usually more than only $3d$ and $2p$ states). Boiling down the full physics to U_{eff} and Δ only, often appears too narrow. In this regard, also a more detailed high- vs- low-energy differentiation governing appears of vital importance.

4 Infinite-layer $NdNiO_2$ system

We focus on the superconducting nickelates and first analyze the $O(2p)$ states in low-valence $NdNiO_2$ at stoichiometry and with finite hole doping. To set the stage, Fig. 2 summarizes the established \mathbf{k} -resolved picture within DFT+sicDMFT^{21,27}. At stoichiometry, $Ni-d_{x^2-y^2}$ is (nearly) Mott-insulating and finite conductivity is (mainly) carried by weakly-filled self-doping bands (cf. Fig. 2a). The latter have mixed character of $Nd(5d)$ as well as $Ni-d_{z^2}$ (around Γ) and $Ni-d_{xz,yz}$ (around A) (see Fig. 2b,e). With hole doping, the flat-band part of $Ni-d_{z^2}$ for $k_z = 1/2$ is shifted towards the Fermi level (cf. Figs. 2d), presumably playing a crucial role in the emergence of superconductivity. This prominent role of the $Ni-d_{z^2}$ flat-band part is similarly revealed in GW+DMFT²⁸. Note that standard DFT+DMFT studies without correlations on oxygen result in weaker correlations for $Ni-d_{x^2-y^2}$, enabling a more cuprate(-like) picture for superconductivity (e.g. Refs. 29, 30). Figure 1 reveals that even with a quite large $\Delta = 5.0$ eV, the hole content h_p amounts to 0.24. The resulting \mathbf{k} -resolved character of the $O(2p)$ states is depicted in Fig. 2c,f. In the stoichiometric case, $O(2p)$ dominated dispersions are easily visible in the energy window $\sim [-10, -5]$ eV. With hole doping, the oxygen p states mix in more strongly near the Fermi level and into the shifted self-doping bands above. For instance around the R point, the flat band at ε_F is a strong mixture of $Ni-d_{x^2-y^2}$, $Ni-d_{z^2}$ and $O(2p)$. Interestingly, the weak $Ni-d_{x^2-y^2}$ low-energy weight in the $k_z = 0$ plane with Γ, X, M is not sizeably hybridized with the p states. This underlines the high- Δ character with seemingly weak Zhang-Rice nature³¹ of its low-energy physics upon hole doping. Weak Zhang-Rice character is also observable in the low-energy part of the \mathbf{k} -integrated spectra, which is displayed in a larger energy range in Figs. 3(a-c). While the small p

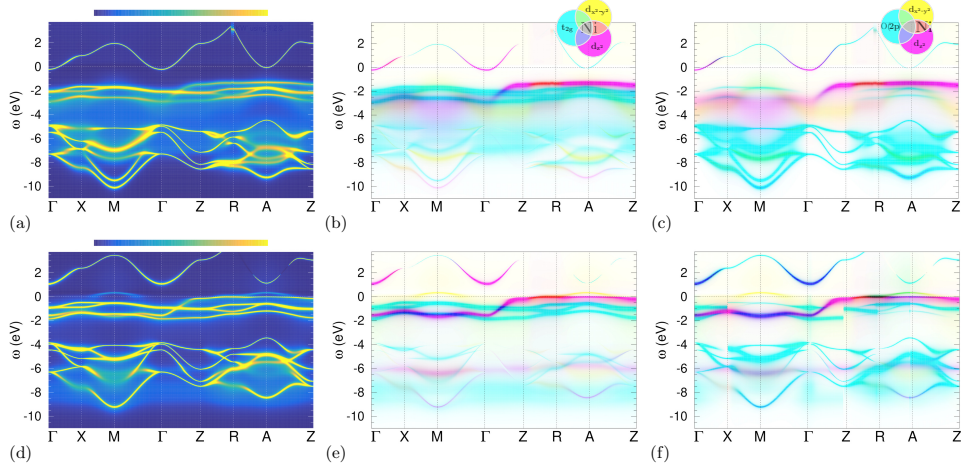


Figure 2. \mathbf{k} -resolved spectral function for stoichiometric NdNiO_2 (a-c) and with 15% hole doping (d-f). (a,d) full $A(\mathbf{k}, \omega)$. (b,e) Fatspec representation resolving $\text{Ni-}d_{x^2-y^2}$ (yellow), $\text{Ni-}d_{z^2}$ (pink) and $\text{Ni-}t_{2g}$ (cyan). (c,f) Same as (b,e) but $\text{Ni-}t_{2g}$ replaced by $\text{O}(2p)$.

weight is comparable to the small d weight at stoichiometry $\delta = 0$ close to the Fermi level, the low-energy d weight strongly dominates over p for finite hole doping δ . Notably, as drawn from the integrated p_z and $(p_x + p_y)$ spectral weight in Figs. 3(d-f), the overall oxygen hole content only increases marginally with substantial hole doping from replacing La by Sr. In other words, most doped holes do not localize on oxygen as in cuprates, but elsewhere, in agreement with electron energy-loss spectroscopy³². In the DFT+sicDMFT

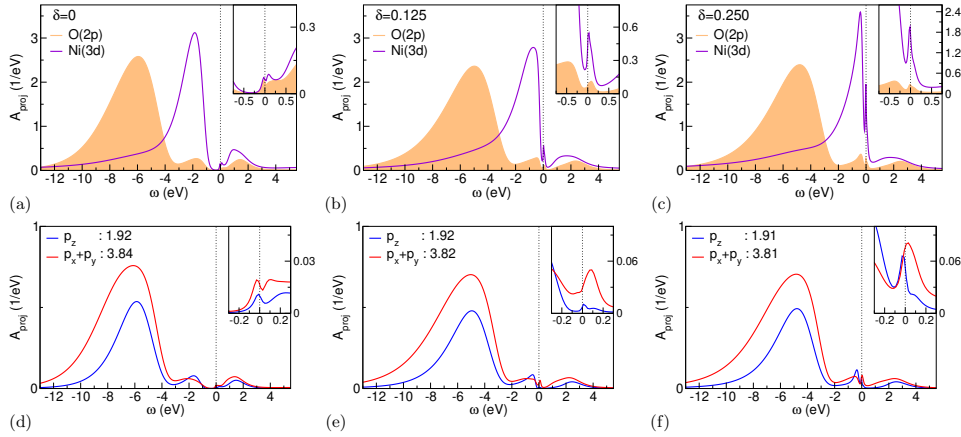


Figure 3. \mathbf{k} -integrated spectral function for stoichiometric NdNiO_2 (a,d), with 12.5% (b,e) and 25% (c,f) hole doping. (a-c) projected $\text{O}(2p)$ and $\text{Ni}(3d)$ spectrum. (d-f) Projected $\text{O-}p_z$ and $\text{O-}(p_x + p_y)$ spectrum, with numbers providing the respective filling.

calculations, doped holes are mostly hosted in the Ni- d_{z^2} orbital²¹. Besides the total $O(2p)$ occupation, a possible asymmetry between p_z and $(p_x + p_y)$ filling may have impact³³. But the data shown in Figs. 3(d-f) show only rather weak asymmetry for the *total* p filling. Yet there is some asymmetry in the low-energy weight, especially with hole doping. For $\delta = 0.125$, the p_z weight close to ε_F is quite small, while for $\delta = 0.25$ it reaches nearly the same value as the one for $(p_x + p_y)$. This may be understandable from the special role of p_z , not meeting a Ni atom in nearest-neighbor distance. For larger δ , low-energy p_z weight becomes more easily coherent with sizeable Ni- d_{z^2} content in the same energy range.

5 $\text{La}_3\text{Ni}_2\text{O}_7$ system

The present challenges of the $\text{La}_3\text{Ni}_2\text{O}_7$ system, representing here the $\text{Ni}(3d^{8-\delta})$ superconducting-nickelate class, are not linked to missing apical oxygens or additional doping features. Here, the sophistication lies in complexities of structural kind and the subtle modifications realized in the high-pressure regime. Canonically, the $\text{La}_3\text{Ni}_2\text{O}_7$ compound is identified as the bilayer, so-called '2222', representative of the m -layered Ruddlesden-Popper series $\text{La}_{m+1}\text{Ni}_m\text{O}_{3m+1}$. Recently, an alternation of mono- and trilayers, so-called '1313', has been found as a competing structural motif³⁴⁻³⁶. The distinct impact of high pressure on the electronic structure is heavily debated. At present, it seems that the (non-)appearance of a Ni- d_{z^2} -based flat band depends on pressure⁸.

Here, we again want to focus on the $O(2p)$ degrees of freedom and their main characteristics in the correlated electronic structure. Nominally, a $\text{Ni}^{7.5}$ filling results from an ionic-limit picture assuming O^{2-} and La^{3+} . However, the charge-transfer energy $\Delta = 3.0$ is comparatively low, and correspondingly, the ligand-hole content $h_p = 0.40$ rather high (see Fig. 1). In general, nickelates with formal oxidation state higher than $\text{Ni}^{2+}(d^8)$ form ligand holes on oxygen to keep an effective Ni^{2+} configuration. From DFT+*sic*DMFT, this is also true for $\text{La}_3\text{Ni}_2\text{O}_7$ with near d^8 filling and one electron/hole in the d_{z^2} and the $d_{x^2-y^2}$ orbital, respectively. Recent experiments³⁷ confirm the theoretical predictions of existing ligand holes. Figures 4(a-c) shows that also the low-energy p -weight is somewhat enhanced compared to the infinite-layer case, though a very strong Zhang-Rice picture as in cuprates does still not emerge. Furthermore, applied pressure appears effective to shift both, main Ni($3d$) and main $O(2p)$ peak to slightly deeper energies in the occupied spectrum.

It proves informative to plot the p_z - and $(p_x + p_y)$ -resolved spectral weight for the different symmetry-inequivalent oxygen sites in the given primitive cells, as done in Figs. 4(d-f). For instance, it may be observed that for all three discussed cases here, i.e. ambient-pressure 2222, high-pressure 2222 and high-pressure 1313, the $p_{x,y}$ orbitals in the LaO flourite block separating the NiO_2 multilayers are responsible for the high-energy ligand-hole peak in the unoccupied spectrum (dashed dark curves from the dark-oxygen-ion symmetry class). One also realizes that the apical oxygens connecting NiO_2 (red-colored ions), here termed bridging (BR) oxygens, show generally the largest energy splitting between p_z and $p_{x,y}$ orbitals. The most interesting behavior is attributed to the low-energy region around the Fermi level, where the p_z orbital of the BR oxygens has apparently a prominent role. Especially for ambient-pressure 2222, the corresponding BR p_z orbital has strongest and peaked spectral weight at ε_F , and furthermore a dominant low-energy ligand-hole weight up to ~ 0.3 eV above the Fermi level (see Fig. 4d). Second in low-energy weight

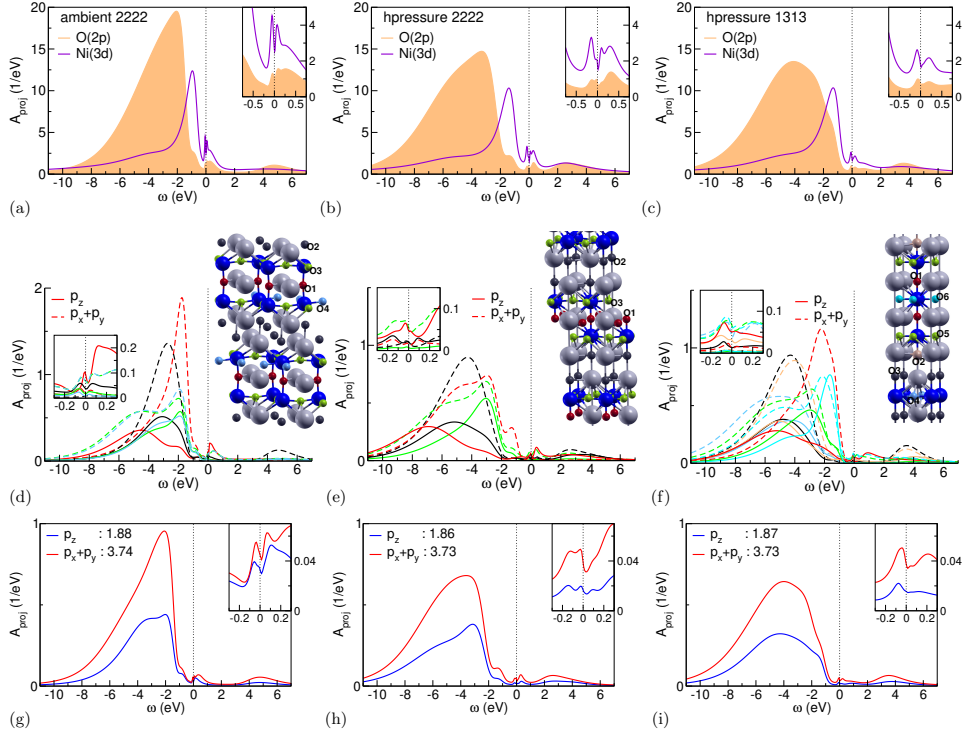


Figure 4. \mathbf{k} -integrated spectral function for $\text{La}_3\text{Ni}_2\text{O}_7$, with La: grey, Ni: darkblue. (a,d,g) 2222 structural motif at ambient pressure and (b,e,f) at high pressure, as well as (c,f,i) 1313 structural motif at high pressure. (a-c) Projected O($2p$) and Ni($3d$) spectrum. (d-f) Projected O- p_z and O- $(p_x + p_y)$ spectrum for symmetry-inequivalent oxygen sites, respectively. (g-i) As (d-f), but summed over all oxygen sites and with numbers providing the respective filling. Note that possible small asymmetries between $p_{x,y}$ are averaged in the plots.

are the in-plane $p_{x,y}$ orbitals (green- and lightblue-colored ions) of the NiO_2 planes, in line with experiment³⁷. Hence there is a quite substantial low-energy asymmetry in favor of p_z within the available O($2p$) states. This finding may be linked to the spin-density-wave transition in ambient-pressure $\text{La}_3\text{Ni}_2\text{O}_7$, which from experiment seems majorly connected to Ni- d_{z^2} involvement³⁸. The p -asymmetry qualitatively still holds at high pressure right at the Fermi level, but is shifted to the higher unoccupied region above ε_F (see Figs. 4e,f). For the 1313 structural motif at high pressure, the p_z orbital of the BR oxygen ion connecting inner at outer layer of the trilayer segment is more low-energy dominant than the one connecting the trilayer with the monolayer segment. When integrating over all symmetry-inequivalent O($2p$) degrees of freedom in Figs. 4(g-i), the discussed asymmetries are mostly evened out, albeit an enhanced p_z low-energy weight is still easily observable for ambient-pressure 2222. A minor slight increase of the total hole content on O($2p$) with pressure may be additionally read off from the data.

6 Concluding Remarks

A detailed inspection of $O(2p)$ degrees of freedom proves useful and necessary for superconducting nickelates, because of their intriguing placement between strong Mott-Hubbard and strong charge-transfer character. Mild orbital asymmetry and lack of significant further oxygen holes upon additional doping are revealed for the infinite-layer systems. On the other hand, a pronounced low-energy p -orbital asymmetry towards the bridging p_z orbital is encountered in the $\text{La}_3\text{Ni}_2\text{O}_7$ system. While some of these observations sound rather subtle, they still may have relevant impact on the low-energy superconductivity phenomenon in these materials. Further work in weighing the relevance of the various site- and orbital sectors in these challenging materials is required.

Acknowledgements

The author thanks N. Poccia, I. M. Eremin and S. Bötzel for helpful discussions. Computations were performed at the Ruhr-University Bochum and the JUWELS Cluster of the Jülich Supercomputing Centre (JSC) under project miqs.

References

1. D. Li, K. Lee, B. Y. Wang, M. Osada, S. Crossley, H. R. Lee, Y. Cui, Y. Hikita, and H. Y. Hwang, *Superconductivity in an infinite-layer nickelate*, *Nature*, **572**, 624, 2019.
2. G. A. Pan, D. F. Segedin, H. LaBollita, Q. Song, E. M. Nica, B. H. Goodge, A. T. Pierce, S. Doyle, S. Novakov, D. C. Carrizales, A. T. N'Diaye, P. Shafer, H. Paik, J. T. Heron, J. A. Mason, A. Jacoby, L. F. Kourkoutis, O. Erten, C. M. Brooks, A. S. Botana, and J. A. Mundy, *Superconductivity in a quintuple-layer square-planar nickelate*, *Nature Materials*, **21**, 160, 2021.
3. H. Sun, M. Huo, X. Hu, J. Li, Y. Han, L. Tang, Z. Mao, P. Yang, B. Wang, J. Cheng, D.-X. Yao, G.-M. Zhang, and M. Wang, *Signatures of superconductivity near 80 K in a nickelate under high pressure*, *Nature*, **621**, 493, 2023.
4. Y. Zhu, D. Peng, E. Zhang, B. Pan, X. Chen, L. Chen, H. Ren, F. Liu, Y. Hao, N. Li, Z. Xing, F. Lan, J. Han, J. Wang, D. Jia, H. Wo, Y. Gu, Y. Gu, L. Ji, W. Wang, H. Gou, Y. Shen, T. Ying, X. Chen, W. Yang, H. Cao, C. Zheng, Q. Zeng, J.-g. Guo, and J. Zhao, *Superconductivity in pressurized trilayer $\text{La}_4\text{Ni}_3\text{O}_{10-\delta}$ single crystals*, *Nature*, **631**, 531, 2024.
5. A.S. Botana, F. Bernardini, and A. Cano, *Nickelate Superconductors: An Ongoing Dialog between Theory and Experiments*, *J. Exp. Theor. Phys.*, **132**, 618, 2021.
6. H. Chen, A. Hampel, J. Karp, F. Lechermann, and A. Millis, *Dynamical mean field studies of infinite layer nickelates: Physics results and methodological implications*, *Front. Phys.*, **10**, 835942, 2022.
7. B. Y. Wang, K. Lee, and B. H. Goodge, *Experimental Progress in Superconducting Nickelates*, *Annu. Rev. Condens. Matter Phys.*, **15**, 305, 2024.
8. M. Wang, H.-H. Wen, T. Wu, D.-X. Yao, and T. Xiang, *Normal and Superconducting Properties of $\text{La}_3\text{Ni}_2\text{O}_7$* , *Chinese Phys. Lett.*, **41**, 077402, 2024.

9. G. Kotliar, S. Y. Savrasov, K. Haule, V. S. Oudovenko, O. Parcollet, and C. A. Marianetti, *Electronic structure calculations with dynamical mean-field theory*, Rev. Mod. Phys., **78**, 865–951, 2006.
10. J. Zaanen, G. A. Sawatzky, and J. W. Allen, *Band gaps and electronic structure of transition-metal compounds*, Phys. Rev. Lett., **55**, 418, 1985.
11. S. Biermann, F. Aryasetiawan, and A. Georges, *First-Principles Approach to the Electronic Structure of Strongly Correlated Systems: Combining the GW Approximation and Dynamical Mean-Field Theory*, Phys. Rev. Lett., **90**, 086402, 2003.
12. L. Boehnke, F. Nilsson, F. Aryasetiawan, and P. Werner, *When strong correlations become weak: Consistent merging of GW and DMFT*, Phys. Rev. B, **94**, 201106, 2016.
13. S. Choi, A. Kutepov, K. Haule, M. van Schilfhaarde, and G. Kotliar, *First-principles treatment of Mott insulators: linearized QSGW+DMFT approach*, npj Quantum Materials, **1**, 16001, 2016.
14. A. van Roekeghem, T. Ayril, J. M. Tomczak, M. Casula, N. Xu, H. Ding, M. Ferrero, O. Parcollet, H. Jiang, and S. Biermann, *Dynamical Correlations and Screened Exchange on the Experimental Bench: Spectral Properties of the Cobalt Pnictide BaCo₂As₂*, Phys. Rev. Lett., **113**, 266403, 2014.
15. W. Körner and C. Elsässer, *First-principles density functional study of dopant elements at grain boundaries in ZnO*, Phys. Rev. B, **81**, 085324, 2010.
16. D. Grieger, C. Piefke, O. E. Peil, and F. Lechermann, *Approaching finite-temperature phase diagrams of strongly correlated materials: A case study for V₂O₃*, Phys. Rev. B, **86**, 155121, 2012.
17. F. Lechermann, W. Körner, D. F. Urban, and C. Elsässer, *Interplay of charge-transfer and Mott-Hubbard physics approached by an efficient combination of self-interaction correction and dynamical mean-field theory*, Phys. Rev. B, **100**, 115125, 2019.
18. C. Elsässer, N. Takeuchi, K. M. Ho, C. T. Chan, P. Braun, and M. Fähnle, *Relativistic effects on ground state properties of 4d and 5d transition metals*, Journal of Physics: Condensed Matter, **2**, no. 19, 4371–4394, May 1990.
19. F. Lechermann, F. Welsch, C. Elsässer, C. Ederer, M. Fähnle, J. M. Sanchez, and B. Meyer, *Density-functional study of Fe₃Al: LSDA versus GGA*, Phys. Rev. B, **65**, 132104, 2002.
20. B. Meyer, C. Elsässer, F. Lechermann, and M. Fähnle, *FORTAN 90 Program for Mixed-Basis-Pseudopotential Calculations for Crystals*, Max-Planck-Institut für Metallforschung, Stuttgart, 1998.
21. F. Lechermann, *Late transition metal oxides with infinite-layer structure: Nickelates versus cuprates*, Phys. Rev. B, **101**, 081110, 2020.
22. P. Werner, A. Comanac, L. de’ Medici, M. Troyer, and A. J. Millis, *Continuous-Time Solver for Quantum Impurity Models*, Phys. Rev. Lett., **97**, 076405, 2006.
23. O. Parcollet, M. Ferrero, T. Ayril, H. Hafermann, I. Krivenko, L. Messio, and P. Seth, *TRIQS: A toolbox for research on interacting quantum systems*, Computer Physics Communications, **196**, 398–415, 2015.
24. P. Seth, I. Krivenko, M. Ferrero, and O. Parcollet, *TRIQS/CTHYB: A continuous-time quantum Monte Carlo hybridisation expansion solver for quantum impurity problems*, Comput. Phys. Commun., **200**, 274–284, 2016.
25. B. Amadon, F. Lechermann, A. Georges, F. Jollet, T. O. Wehling, and A. I. Licht-

- enstein, *Plane-wave based electronic structure calculations for correlated materials using dynamical mean-field theory and projected local orbitals*, Phys. Rev. B, **77**, 205112, 2008.
26. V. Bisogni, S. Catalano, R. J. Green, M. Gibert, R. Scherwitzl, Y. Huang, V. N. Strocov, P. Zubko, S. Balandeh, J.-M. Triscone, G. Sawatzky, and T. Schmitt, *Ground-state oxygen holes and the metal–insulator transition in the negative charge-transfer rare-earth nickelates*, Nature Communications, **7**, 13017, 2016.
 27. F. Lechermann, *Doping-dependent character and possible magnetic ordering of NdNiO₂*, Phys. Rev. Mater., **5**, 044803, 2021.
 28. F. Petocchi, V. Christiansson, F. Nilsson, F. Aryasetiawan, and P. Werner, *Normal State of Nd_{1-x}Sr_xNiO₂ from Self-Consistent GW + EDMFT*, Phys. Rev. X, **10**, 041047, 2020.
 29. M. Kitatani, L. Si, O. Janson, R. Arita, Z. Zhong, and K. Held, *Nickelate superconductors—a renaissance of the one-band Hubbard model*, npj Quantum Mater., **5**, 59, 2020.
 30. J. Karp, A. S. Botana, M. R. Norman, H. Park, M. Zingl, and A. Millis, *Many-Body Electronic Structure of NdNiO₂ and CaCuO₂*, Phys. Rev. X, **10**, 021061, 2020.
 31. F. C. Zhang and T. M. Rice, *Effective Hamiltonian for the superconducting Cu oxides*, Phys. Rev. B, **37**, 3759, 1988.
 32. B. H. Goodge, D. Li, K. Lee, M. Osada, B. Y. Wang, G. A. Sawatzky, H. Y. Hwang, and L. F. Kourkoutis, *Doping evolution of the Mott–Hubbard landscape in infinite-layer nickelates*, PNAS, **118**, e2007683118, 2021.
 33. A. Bianconi, M. De Santis, A. Di Cicco, A. M. Flank, A. Fontaine, P. Lagarde, H. Katayama-Yoshida, A. Kotani, and A. Marcelli, *Symmetry of the 3d⁹ ligand hole induced by doping in YBa₂Cu₃O_{7-δ}*, Phys. Rev. B, **38**, 7196, 1988.
 34. X. Chen, J. Zhang, A. S. Thind, S. r Sharma, H. LaBollita, G. Peterson, H. Zheng, D. P. Phelan, A. S. Botana, R. F. Klie, and J. F. Mitchell, *Polymorphism in the Ruddlesden–Popper Nickelate La₃Ni₂O₇: Discovery of a Hidden Phase with Distinctive Layer Stacking*, J. Am. Chem. Soc., **146**, no. 6, 3640, 2024.
 35. P. Puphal, P. Reiss, N. Enderlein, Y.-M. Wu, G. Khaliullin, V. Sundaramurthy, T. Priessnitz, M. Knauff, A. Suthar, L. Richter, M. Isobe, P. A. van Aken, H. Takagi, B. Keimer, Y. E. Suyolcu, B. Wehinger, P. Hansmann, and M. Hepting, *Unconventional Crystal Structure of the High-Pressure Superconductor La₃Ni₂O₇*, Phys. Rev. Lett., **133**, 146002, 2024.
 36. H. Wang, L. Chen, A. Rutherford, H. Zhou, and W. Xie, *Long-Range Structural Order in a Hidden Phase of Ruddlesden–Popper Bilayer Nickelate La₃Ni₂O₇*, Inorganic Chemistry, **63**, no. 11, 5020–5026, 2024.
 37. Z. Dong, M. Huo, J. Li, J. Li, P. Li, H. Sun, L. Gu, Y. Lu, M. Wang, Y. Wang, and Z. Chen, *Visualization of oxygen vacancies and self-doped ligand holes in La₃Ni₂O_{7-δ}*, Nature, **630**, 847, 2024.
 38. X. Chen, J. Choi, Z. Jiang, J. Mei, K. Jiang, J. Li, S. Agrestini, M. Garcia-Fernandez, X. Huang, H. Sun, D. Shen, M. Wang, J. Hu, Y. Lu, K.-J. Zhou, and D. Feng, *Electronic and magnetic excitations in La₃Ni₂O₇*, arXiv:2401.12657, 2024.